

# New algorithm of measuring gravitational wave radiation from rotating binary system

Soon-Tae Hong\*

*Center for Quantum Spacetime and Department of Physics, Sogang University, Seoul 04107, Korea*

(Dated: September 4, 2024)

In order to investigate the gravitational wave (GW) radiation, without resorting to the traceless transverse gauge approach to the GW formalism of the linearized general relativity, we formulate the so-called modified linearized general relativity (MLGR). As an application of the MLGR, we construct a novel paradigm of measuring the GW radiation from a binary system of compact objects, to theoretically interpret its phenomenology. To accomplish this, we formulate the mass scalar and mass vector potentials for the merging binary compact objects, from which we construct the mass magnetic field in addition to the mass electric one which also includes the mass vector potential effect. Next, defining the mass Poynting vector in terms of the mass electric and mass magnetic fields in the MLGR, we find the GW radiation intensity profile possessing a prolate ellipsoid geometry due to the merging binary compact objects source. At a given radial distance from the binary compact objects, the GW radiation intensity on the revolution axis of the binary compact objects is shown to be twice that on the equatorial plane. Moreover, we explicitly obtain the total radiation power of the GW, which has the same characteristic as that of the electromagnetic wave in the rotating charge electric dipole moment. We also find that, in no distorting limit of the merging binary compact objects, the compact objects in the MLGR do not yield the total GW radiation power, consistent with the result of the traceless transverse gauge algorithm in the linearized general relativity.

**Keywords:** gravitational wave radiation; modified linearized general relativity; merging binary compact objects; mass Poynting vector; distortion

## I. INTRODUCTION

The linearized general relativity (LGR) [1–3] has been investigated to describe the gravitational wave (GW) radiation from a binary system of compact objects (namely stars or black holes) for instance. To be specific, in order to study the physical phenomenology in the LGR, we need to assume that the gravity fields are weak so that the gravitational field equations can be linearized. Next it is well known that, in vacuum of the LGR, the binary compact objects oscillating in time emit spin-two gravitons which are quanta of the GW. Mathematically the spin-two gravitons originate from the second rank tensor associated with the curved spacetime metric  $g_{\alpha\beta}$  [4]. In order to construct the GW which is transverse to the GW propagating direction and yields the spin-two graviton, we have exploited the traceless transverse (TT) gauge [1–3]. In contrast, the spin-one photons which are quanta of the electromagnetic (EM) wave in vacuum are delineated in terms of the vectorial quantities of the charge scalar and charge vector potentials defined in the flat spacetime.

On the other hand, since the first GW was detected by Advanced LIGO [5], there have been lots of progresses in an observational astrophysics. In particular, the third generation network of ground-based detectors [6] is currently proposed to obtain improved sensitivities, compared to those of the Advanced LIGO detector. Recently, the GW from neutron star and black hole has been observed [7], and the galaxy-based observatories have been proposed [8]. In order to constrain cosmology, a theoretical probe of cosmology which exploits population level properties of lensed GW detections has been also proposed [9]. Next, since the gamma ray burst (GRB) discovery was published [10], to elucidate the GRB associated with the magnetar (namely highly-magnetized neutron star) for instance [11], we have observed many theoretical models including the Dirac type relativistic massive photon model [12], where the anti-photon corresponding to the negative energy solution is proposed as a candidate for an intense radiation flare of the GRB. The GW detector network has observed the GW merger event originating from binary neutron star GW170817 in 2017 [13–15]. Note that the GW170817 merger event has been known to be consistent with the GRB of GRB170817A [14, 15]. To be specific, the GW is supposed to be produced from neutron star oscillations related with magnetar giant flares and the corresponding GRB [16].

In this paper, we will propose a new theoretical paradigm of the modified linearized general relativity (MLGR), in which we will formulate the Green retarded [1, 2] mass scalar and mass vector potentials of a binary system of compact objects. Using these potentials in the MLGR, we will next construct the mass electric and mass magnetic

---

\*Electronic address: galaxy.mass@gmail.com

fields. In particular, in order to formulate the non-vanishing mass magnetic field, we will introduce the distortion of the spirally merging binary compact objects during one cycle of their revolution. Making use of the mass electric and mass magnetic fields, we will find the mass Poynting vector which is exploited to construct a theoretical scheme of measuring the GW radiation from a binary system of compact objects. Moreover, introducing the TT gauge, we will study the GW of the binary compact objects in the LGR.

In Section 2 we will formulate the LGR and MLGR algorithms. In Section 3, as an application of the MLGR, we will investigate the phenomenology of the merging binary compact objects. To do this, we will explicitly formulate the physical quantities such as the mass scalar and mass vector potentials, and the mass Poynting vector. We will also study the TT gauge in the LGR. Section 4 includes conclusions. In Appendix A, we will briefly study the EM radiation from the rotating charge electric dipole moment. In Appendix B, we will briefly comment on the TT gauge formalism for the gravitation radiation from the rotating mass compact objects. In Appendix C, we will also address comments on the formalism of massive spin-one graviton.

## II. SET UP OF LGR AND MLGR ALGORITHMS

### A. LGR algorithm

Now we will study the LGR [1–3]. To accomplish this, we first assume that the deviation  $h_{\alpha\beta}$  of the spacetime metric  $g_{\alpha\beta}$  from a flat metric  $\eta_{\alpha\beta}$  is small:  $g_{\alpha\beta} = \eta_{\alpha\beta} + h_{\alpha\beta}$ . After some algebra we find the linearized Einstein equation [1]

$$-\frac{1}{2}\square\bar{h}_{\alpha\beta} + \partial^\gamma\partial_{(\alpha}\bar{h}_{\beta)\gamma} - \frac{1}{2}\eta_{\alpha\beta}\partial^\gamma\partial^\delta\bar{h}_{\gamma\delta} = \frac{8\pi G}{c^4}T_{\alpha\beta}, \quad (2.1)$$

where  $\square = \partial^\beta\partial_\beta$  with the metric  $(-1, +1, +1, +1)$ , and  $T_{\alpha\beta}$  is the energy stress tensor. Here the trace reversed perturbation  $\bar{h}_{\alpha\beta}$  is given by  $\bar{h}_{\alpha\beta} = h_{\alpha\beta} - \frac{1}{2}\eta_{\alpha\beta}h$  and  $h = \eta^{\alpha\beta}h_{\alpha\beta}$ . Exploiting (2.1) and the Lorentz gauge condition (LGC) in the gravity

$$\partial^\beta\bar{h}_{\alpha\beta} = 0, \quad (2.2)$$

we arrive at

$$\square\bar{h}_{\alpha\beta} = -\frac{16\pi G}{c^4}T_{\alpha\beta}. \quad (2.3)$$

Next we use the fact that the LGC in (2.2) is preserved by the gauge transformation

$$h_{\alpha\beta} \rightarrow h'_{\alpha\beta} = h_{\alpha\beta} + \partial_\alpha\xi_\beta + \partial_\beta\xi_\alpha, \quad (2.4)$$

if the following restricted gauge freedom condition is exploited [1]

$$\square\xi_\alpha = 0. \quad (2.5)$$

In other words, using the relation

$$\partial^\beta\bar{h}_{\alpha\beta} \rightarrow \partial^\beta\bar{h}'_{\alpha\beta} = \partial^\beta\bar{h}_{\alpha\beta} + \square\xi_\alpha. \quad (2.6)$$

we find that, to preserve the LGC of  $\partial^\beta\bar{h}'_{\alpha\beta} = 0$  in (2.6) in the LGR, we need to ensure that  $\square\xi_\alpha = 0$  as shown in (2.5).

Now we address brief comments on the radiation gauge, and the corresponding initial value problem and dynamics of the massive spin-two graviton [1–3]. First, in a source free region possessing  $T_{\alpha\beta} = 0$  in the LGR, (2.3) becomes

$$\square\bar{h}_{\alpha\beta} = 0. \quad (2.7)$$

Next we use the radiation gauge [1, 2]

$$h = 0, \quad h_{0i} = 0 \quad (i = 1, 2, 3), \quad (2.8)$$

to yield [1, 2]

$$\bar{h}_{\alpha\beta} = h_{\alpha\beta}, \quad (2.9)$$

and

$$h_{00} = 0. \quad (2.10)$$

To find the radiation gauge in (2.8), on the initial surface  $t = t_0$  we need to exploit (2.4). For instance, the conditions  $h' = 0$  and  $h'_{0i} = 0$  yield

$$\begin{aligned} -h &= 2 \left( -\frac{\partial \xi_0}{\partial t} + \nabla \cdot \vec{\xi} \right), \\ -h_{0i} &= \frac{\xi_i}{\partial t} + \frac{\xi_0}{\partial x^i}, \end{aligned} \quad (2.11)$$

where  $\xi_\alpha = (\xi_0, \xi_i)$  ( $\alpha = 0, 1, 2, 3$ ). Next the first time derivatives of (2.11) produce

$$\begin{aligned} -\frac{\partial h}{\partial t} &= 2 \left( -\nabla^2 \xi_0 + \nabla \cdot \frac{\partial \vec{\xi}}{\partial t} \right), \\ -\frac{\partial h_{0i}}{\partial t} &= \nabla^2 \xi_i + \frac{\partial}{\partial x^i} \left( \frac{\xi_0}{\partial t} \right). \end{aligned} \quad (2.12)$$

Note that exploiting (2.11) and (2.12) we obtain the inertial values of  $\xi_\alpha$  ( $\alpha = 0, 1, 2, 3$ ) and their first time derivatives, and thus we define  $\xi_\alpha$  to be the solution of (2.5) with these initial data [1].

Second, exploiting  $\bar{h}_{\alpha\beta} = h_{\alpha\beta}$  in (2.9) related with the radiation gauge in (2.8) the source free linearized Einstein equation produces plane GW solution of the form [1–3]

$$h_{\alpha\beta} = H_{\alpha\beta} e^{ik_\mu x^\mu}, \quad (2.13)$$

where  $H_{\alpha\beta}$  is a constant symmetric second rank tensor field and  $k^\mu$  is the GW four-vector. Note that the symmetric tensor  $H_{\alpha\beta}$  ( $= H_{\beta\alpha}$ ) has ten different components. However the four LGCs in (2.2) reduce the number of independent degrees of freedom (DOF) to six. Moreover the four gauge transformation conditions in (2.5) reduce the six independent components to two DOF which implies that we find two possible polarizations for the spin-two plane GW in (2.13) [1, 2].

Third, we study the spin-two plane GW in the vacuum having  $T_{\alpha\beta} = 0$ . Inserting  $h_{\alpha\beta}$  in (2.13) into (2.7), we find that the GW four-vector  $k^\mu$  satisfies

$$k_\mu k^\mu = 0, \quad (2.14)$$

to yield, for the plane GW traveling in the  $z$  direction,

$$k^\mu = (k, 0, 0, k). \quad (2.15)$$

Next, combining  $h_{\alpha\beta}$  in (2.13) and the LGC in (2.2), we obtain the transversality condition for the symmetric second rank tensor  $H_{\mu\nu}$

$$k^\mu H_{\mu\nu} = 0. \quad (2.16)$$

The aspects associated with (2.14)–(2.16) imply that a massless spin-two field propagates with speed of light in flat spacetime [4] and its quantized objects are spin-two gravitons possessing the two transverse polarization DOF. Inserting the GW solution in (2.13) into (2.8) and (2.10) we arrive at [1]

$$\eta^{\mu\nu} H_{\mu\nu} = 0, \quad H_{0\mu} = 0, \quad (\mu = 0, 1, 2, 3). \quad (2.17)$$

Fourth, similar to the case of the massive photon [12], we find the relation for the *massive* spin-two graviton

$$k^\mu H_{\mu\nu} \neq 0, \quad (2.18)$$

since for the massive spin-two graviton we have longitudinal component in addition to transverse ones, as in the case of the phonon associated with massive particle lattice vibrations [17]. In other words, the massive spin-two graviton has three components to yield three DOF. Note that, as in the case of the GRB in the Dirac type relativistic massive photon model [12], the massive spin-two graviton could be interpreted as a spin-two GRB-like particle.

## B. MLGR algorithm

Now, we will formulate the MLGR which includes explicitly the mass current DOF. As a model appropriate for the GW radiation from rotating binary system, we propose the MLGR where we have the non-vanishing  $\bar{h}^{00}$  and  $\bar{h}^{0i}$  ( $i = 1, 2, 3$ ), together with

$$\bar{h}^{ij} = 0. \quad (2.19)$$

Note that the TT gauge of the LGR related with the GW radiation will be briefly discussed in the ensuing section and Appendix B.

Next we define in the MLGR the time-time component of the trace reversed perturbation  $\bar{h}^{00}$  and the corresponding energy stress tensor  $T^{00}$  as

$$\bar{h}^{00} = -\frac{4}{c}A_M^0, \quad T^{00} = c^2\rho_M, \quad (2.20)$$

where  $\rho_M$  is the mass density. Here the subscript  $M$  denotes the mass related quantities and will be applied to the gravitational interaction physical quantities from now on. Inserting (2.20) into (2.3) yields

$$\square A_M^0 = \frac{4\pi G}{c}\rho_M, \quad (2.21)$$

implying that we have the dynamical DOF in the MLGR.

Making use of the definition  $\phi_M \equiv cA_M^0$  and (2.20), we find

$$\bar{h}^{00} = -\frac{4}{c^2}\phi_M, \quad (2.22)$$

and, in the static limit, (2.21) produces

$$\nabla^2\phi_M = 4\pi G\rho_M, \quad (2.23)$$

which is in agreement with the Newtonian gravity [1, 18]. In contrast, in the TT gauge we find  $\bar{h}_{TT}^{00} = 0$  in (3.17) implying that this gauge is not simultaneously applicable to the Newtonian gravity.

Next in the MLGR we define the time-space components of the trace reversed perturbation  $\bar{h}^{0i}$  and the energy stress tensor  $T^{0i}$  as

$$\bar{h}^{0i} = -\frac{4}{c}A_M^i, \quad T^{0i} = cJ_M^i, \quad (2.24)$$

where  $J_M^i \equiv \rho_M v^i$  is the *non-vanishing mass current density* associated with the velocity  $v^i$  of the mass density [1]. To be more specific, we investigate the predictions of the linearized gravity when the *lowest order effects* of the motion of sources are taken into account. In this approximation, we proceed to neglect stresses to yield the energy stress tensor of the form [1]

$$T_{\alpha\beta} = 2t_{(\alpha}J_{\beta)} - c^2\rho_M t_\alpha t_\beta, \quad (2.25)$$

where  $t^\alpha = (\partial/\partial x^0)^\alpha$  is the time direction of the coordinate system and  $J_\beta = -T_{\alpha\beta}t^\alpha$  is mass energy current density four-vector. Note that, in this Wald approximation in the MLGR, we find  $J_\alpha = \rho_M u_\alpha$  with  $u^\alpha = (c, v^i)$ . Maintaining the Wald idea associated with (2.25), we construct  $T^{\alpha\beta}$  in terms of  $J_M^i = \rho_M v^i$  which is linear order in  $v^i$

$$T^{\alpha\beta} = \begin{pmatrix} c^2\rho_M & cJ_M^j \\ cJ_M^i & 0 \end{pmatrix} \quad (2.26)$$

which reproduces  $T^{00}$  and  $T^{0i}$  in (2.20) and (2.24). Note that the space-space component  $T^{ij}$  in (2.26) vanishes as expected, and the corresponding  $\bar{h}^{ij}$  vanishes as in (2.19) in the Wald approximation. Note also that this energy stress tensor has been used in the Newtonian gravity in (2.23) for the case of  $T^{00} = c^2\rho_M$ . In the ensuing section the Wald approximation also will be exploited in the gravitational wave radiation from rotating binary system where the corresponding compact object mass moves with  $J_M^i = \rho_M v^i$  where  $v^i$  is given by *non-vanishing velocity*  $(v^i v^i)^{1/2} = a\omega$  along the tangential direction to the circular orbit of radius  $a$  as shown in Figure 1(a). Here  $\omega$  is angular frequency of the mass. In this work we will thus make use of the Wald approximation in the MLGR in the gravitational wave radiation phenomenology.

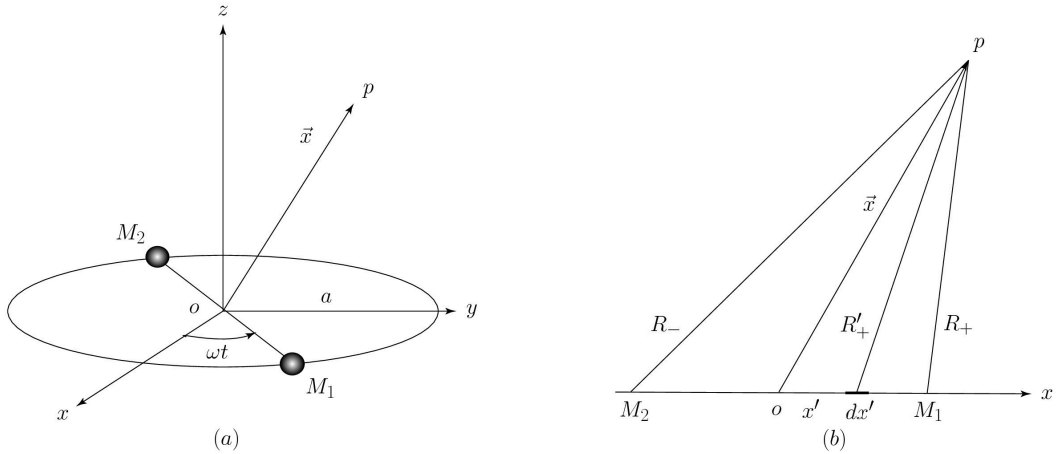


FIG. 1: (a) The schematic diagram for a binary system of compact objects  $M_1$  and  $M_2$  of equal mass  $M$  which co-rotate in circular orbits of radius  $a$  about their common center of mass  $o$  located at the origin, with an angular frequency  $\omega$ . (b) The diagram for the geometry of  $R_{\pm}$  for the retarded mass scalar potentials  $\phi_M^I$  in (3.2) and  $R'_+$  for the retarded mass vector potentials  $\vec{A}_M^I$  in (3.6). Here  $\vec{x} = r(\hat{x} \sin \theta \cos \phi + \hat{y} \sin \theta \sin \phi + \hat{z} \cos \theta)$  denotes a radial vector from the origin  $o$  to an observation point.

In the MLGR, inserting (2.24) into (2.3) produces

$$\square A_M^i = \frac{4\pi G}{c^2} J_M^i. \quad (2.27)$$

Combining (2.21) and (2.27), we find the covariant form of the equations of motion

$$\square A_M^\alpha = \frac{4\pi G}{c^2} J_M^\alpha, \quad (2.28)$$

where  $A_M^\alpha = \left( \frac{\phi_M}{c}, A_M^i \right)$  and the four mass current density is defined by  $J_M^\alpha = (c\rho_M, J_M^i)$ . Note that the LGC in (2.2) is rewritten as

$$\partial_\alpha A_M^\alpha = 0. \quad (2.29)$$

Exploiting  $A_M^\alpha$  in (2.20) and (2.24), we find

$$A_M^\alpha = -\frac{c}{4} \bar{h}^{0\alpha}, \quad (2.30)$$

to yield the equation of motion

$$\square \bar{h}^{0\alpha} = -\frac{16\pi G}{c^3} J_M^\alpha. \quad (2.31)$$

Note that the LGC in (2.29) becomes

$$\partial_\alpha \bar{h}^{0\alpha} = 0. \quad (2.32)$$

Next in the EM phenomenology we obtain the equation of motion

$$\square A_Q^\alpha = -\frac{1}{c^2 \epsilon_0} J_Q^\alpha, \quad (2.33)$$

where  $A_Q^\alpha = \left( \frac{\phi_Q}{c}, A_Q^i \right)$  and  $J_Q^\alpha = (c\rho_Q, J_Q^i)$ . Here the minus sign in (2.33) denotes that the EM interaction is repulsive and the *spin-one* photon mediates repulsive charges. Next the plus sign in (2.28) implies that the gravity interaction is attractive. Moreover, exploiting the mathematical structures of the equations of motion of  $A_Q^\alpha$  and  $A_M^\alpha$ , we find that the *spin-one* graviton mediates attractive masses. In other words, to treat the *spin-one* graviton in the Wald approximation in the MLGR, we use the vectorial algorithm in (2.28), which is similar to the EM phenomenology discussed in (2.33). Note that in the LGR having the tensorial non-vanishing  $h_{ij}$  ( $i, j = 1, 2, 3$ ) there exists no *spin-one*

graviton DOF [1]. To be more specific, in the LGR the gauge transformation is given by (2.4) which has the Lie derivative  $\mathcal{L}_\xi \eta_{\alpha\beta} = \partial_\alpha \xi_\beta + \partial_\beta \xi_\alpha$ . In contrast, we cannot introduce this kind of second rank tensorial form in the gauge transformation in the MLGR.<sup>1</sup> Instead, motivated by the mathematical similarity in the vectorial forms of the equations of motion for  $A_M^\alpha$  ( $= -\frac{c}{4} \bar{h}^{0\alpha}$ ) ( $\alpha = 0, 1, 2, 3$ ) in (2.28) and  $A_Q^\alpha$  in (2.33), we make use of the *vectorial* gauge transformation

$$\bar{h}_{0\alpha} \rightarrow \bar{h}'_{0\alpha} = \bar{h}_{0\alpha} + \partial_\alpha \psi, \quad (2.34)$$

which is *analogous* to that in the EM phenomenology [1, 19] possessing two transverse polarization DOF of the spin-one photon and the vectorial gauge transformation

$$A_Q^\alpha \rightarrow A_Q^{\alpha'} = A_Q^\alpha + \partial^\alpha \zeta. \quad (2.35)$$

These features imply that, in the Wald approximation in the MLGR, the graviton also has spin-one and the corresponding two transverse polarization DOF. Note that in the LGR we find the spin-two graviton having two transverse polarization DOF in the previous subsection.

Now we investigate the GW defined in the vacuum. To accomplish this, inserting  $J_M^\alpha = 0$  into (2.31) and exploiting  $\bar{h}^{0\alpha}$  in (2.30), we obtain the wave equation for the non-vanishing field  $\bar{h}^{0\alpha}$  (or  $A_M^\alpha$ )

$$\square \bar{h}^{0\alpha} = \square A_M^\alpha = 0. \quad (2.36)$$

Note that the wave equations in (2.36) in the MLGR describe a massless spin-one graviton propagating in the flat spacetime, similar to a massless spin-one photon propagating in the flat spacetime. In other words, (2.36) explains the spin-one gravitons of gravitational field.

Next it seems appropriate to comment on the spin of the graviton in the MLGR. In vacuum with  $T_{\alpha\beta} = 0$  in (2.3), we end up with the wave equation  $\square \bar{h}_{\alpha\beta} = 0$  which *could* describe a massless spin-two graviton propagating in the flat spacetime [4]. However, if we consider only the *physically meaningful wave equation* for  $A_M^\alpha$  in (2.36) obtained from that for  $\bar{h}^{0\alpha}$  ( $\alpha = 0, 1, 2, 3$ ), we mathematically find a massless spin-one graviton whose properties are well defined in the MLGR. Note that the condition  $\bar{h}^{ij} = 0$  in (2.19) reduces the number of independent components of  $\bar{h}^{\alpha\beta}$  to four. The *independent* components ( $\bar{h}^{00}, \bar{h}^{0i}$ ) thus correspond to the four components of  $A_M^\alpha$ . Next we explicitly find the solution of the GW field equation in (2.36) as follows

$$\bar{h}^{0\alpha} = \epsilon^\alpha e^{ik_\mu x^\mu}, \quad (2.37)$$

where  $k^\mu$  is the GW four-vector. Here  $\epsilon^\alpha$  is the constant amplitude vector corresponding to the GW polarizations.

Now we find that, similar to (2.35) in the EM formalism, the LGC in (2.32) is preserved by the gauge transformation in (2.34) in the Wald approximation in the MLGR if

$$\square \psi = 0. \quad (2.38)$$

Making use of the relation

$$\partial^\alpha \bar{h}_{0\alpha} \rightarrow \partial^\alpha \bar{h}'_{0\alpha} = \partial^\alpha \bar{h}_{0\alpha} + \square \psi. \quad (2.39)$$

we observe that, to preserve the LGC of  $\partial^\beta \bar{h}'_{\alpha\beta} = 0$  in (2.39) in the MLGR, we need to ensure that  $\square \psi = 0$  as shown in (2.38). Note that the LGC in (2.32) in the MLGR has the same structure as the LGC in the electromagnetism. Note also that the polarization vector  $\epsilon^\alpha$  has four different components. However the one LGC in (2.32) reduces the number of independent DOF to three. Next the one gauge transformation condition in (2.38) reduces the three independent components to two DOF which implies that we obtain two possible polarizations for the spin-one plane GW in (2.37). Note that the gauge choices (2.32) and (2.38) in the MLGR determine the fundamental nature of the DOF to yield two transverse polarizations, as in the gauge choices in (2.2) and (2.5) in LGR where we also have two transverse polarizations.

Next we study the radiation gauge, and the corresponding initial value problem and dynamics of the massless spin-one graviton whose mathematical structure is the same as the massless photon. For the case of massive spin-one

---

<sup>1</sup> In the Wald approximation in the MLGR, there is no way to define the tensorial gauge transformation for the non-vanishing  $\bar{h}_{0i}$  ( $i = 1, 2, 3$ ), since the radiation gauge in the LGR having the tensorial gauge transformation in (2.4) already possesses the vanishing components  $\bar{h}_{0i} = h_{0i} = 0$  in (2.8) for instance. To circumvent this difficulty, in the Wald approximation we exploit the vectorial gauge transformation in (2.34).

graviton, see below (2.49). Treating the spin-one GW, we exploit the gauge DOF in a source free region having  $J_M^\alpha = 0$  by using the radiation (or Coulomb) gauge [1, 19]. On a constant time surface  $t = t_0$  of the global inertial coordinate system we need to solve

$$\partial^i \bar{h}_{0i} + \nabla^2 \psi = 0. \quad (2.40)$$

We define  $\psi$  throughout spacetime to be the solution of (2.38) whose initial value on the time surface  $t = t_0$  is given by (2.40). Moreover the time derivative of  $\psi$  is given by

$$\bar{h}_{00} + \frac{\partial \psi}{\partial t} = 0. \quad (2.41)$$

The function defined as

$$F \equiv \bar{h}_{00} + \frac{\partial \psi}{\partial t} \quad (2.42)$$

then satisfies the inhomogeneous equation of motion including the gauge DOF

$$\square F = -\frac{16\pi G}{c^3} J_M^0. \quad (2.43)$$

Moreover on the initial surface  $t = t_0$  we find

$$F = 0, \quad \frac{\partial F}{\partial t} = \partial_i \bar{h}_{0i} + \nabla^2 \psi. \quad (2.44)$$

Note that, for the inhomogeneous equation of motion having  $J_M^\alpha \neq 0$  ( $\alpha = 0, 1, 2, 3$ ) associated with mass  $M$ , see the ensuing section where  $\bar{h}^{0\alpha} (= -\frac{4}{c} A_M^\alpha)$ , and the corresponding mass electric and mass magnetic fields  $\vec{E}_M$  and  $\vec{B}_M$  in (3.11) will be explicitly evaluated. Moreover the directions of  $\vec{E}_M$  and  $\vec{B}_M$  will be shown to represent the two transverse directions of GW. In this formulation we do not need the remnant components  $\bar{h}^{ij}$  in (2.19) which are unnecessary in the *photon-like* spin-one graviton algorithm having the mass scalar and mass vector potentials  $A_M^\alpha = (\frac{1}{c} \phi_M, A_M^i)$ . Note also that, for the case of the inhomogeneous equation of motion possessing  $\rho_M \neq 0$  only which is related with mass  $M$  in the TT gauge in the LGR, see Appendix B where we will formulate the quadrupole moment tensor  $I^{ij}$  and the corresponding second rank tensor  $\bar{h}_{TT}^{ij}$  in (B.8).

Inserting (2.37) into (2.36), we find  $k_\mu k^\mu = 0$  to yield

$$k^\mu = (k, 0, 0, k), \quad (2.45)$$

which describes the massless spin-one graviton. Making use of (2.37) and the LGC in (2.32), we obtain

$$k_\mu \epsilon^\mu = 0, \quad (2.46)$$

to produce  $\epsilon^0 = \epsilon^3$ . Note that the polarization vector  $\epsilon^\alpha$  satisfies the transversality condition in (2.46), which is needed since the massless spin-one graviton possesses the transverse components only. Note also that, in the LGR related with  $h_{\alpha\beta}$  in (2.13) satisfying the LGC in (2.2), we find the transversality condition  $k^\mu H_{\mu\nu} = 0$  in (2.16) for the symmetric second rank tensor  $H_{\mu\nu}$ .

Next we assume  $\psi = \epsilon e^{ik_\mu x^\mu}$  and  $\bar{h}'^{0\alpha} = \epsilon'^\alpha e^{ik_\mu x^\mu}$  in the Wald approximation in the MLGR, and then we exploit the gauge transformation equation  $\bar{h}'^{0\alpha} = \bar{h}^{0\alpha} + \partial^\alpha \psi$  to yield

$$\epsilon'^\alpha = \epsilon^\alpha + i\epsilon k^\alpha. \quad (2.47)$$

Using (2.45) and (2.47), we explicitly find the non-trivial relation  $\epsilon'^0 = \epsilon^0 + i\epsilon k$ . Next, exploiting the ansatz  $\epsilon = \frac{i}{k} \epsilon^0$ , we find  $\epsilon'^0 = 0$ . Dropping the primes in  $\epsilon'^\alpha$  we obtain

$$\epsilon^\alpha = (0, \epsilon^1, \epsilon^2, 0), \quad (2.48)$$

implying that the GW is transverse to the propagation direction  $k^\alpha$  in (2.45). Note that  $\epsilon^\alpha$  in (2.48) thus satisfies the identity  $\epsilon^\alpha k_\alpha = 0$  in (2.46) as expected.

Now we have comments on the GW phenomenology in terms of  $\epsilon^\alpha$  in (2.48) in the Wald approximation in the MLGR. First, in the cases of  $\epsilon^\alpha = (0, \epsilon^1, 0, 0)$  and  $\epsilon^\alpha = (0, 0, \epsilon^2, 0)$ , as the GW passes a free test particle, the test particle will oscillate in the  $x$  and  $y$  directions with a magnitude changing sinusoidally with time, respectively,

following the GW wave relation in (2.37). Second, in the cases of  $\epsilon^\alpha = (0, \epsilon^1, i\epsilon^1, 0)$  and  $\epsilon^\alpha = (0, \epsilon^1, -i\epsilon^1, 0)$ , the GW polarizations yield left-circularly and right-circularly polarized GWs, and then the test particle will move in the corresponding circles, respectively. Third, in the general cases of  $\epsilon^\alpha = (0, \epsilon^1, i\bar{\epsilon}^1, 0)$  and  $\epsilon^\alpha = (0, \epsilon^1, -i\bar{\epsilon}^1, 0)$  ( $\epsilon^1 \neq \bar{\epsilon}^1$ ), the GW polarizations produce left-elliptic and right-elliptic polarized GWs, respectively, and thus the test particle will move in the corresponding ellipses.

Next we investigate the properties of the massive graviton in the Wald approximation in the MLGR. As in the case of the massive photon [12], we find the identity

$$k_\mu \epsilon^\mu \neq 0, \quad (2.49)$$

for the massive graviton, since for the massive graviton we have longitudinal component in addition to transverse ones, similar to the phonon associated with massive particle lattice vibrations [17]. Namely, the massive spin-one graviton has three components to produce three DOF, similar to the massive photon and to the massive spin-two graviton. Note that the dynamics of the massive spin-one graviton are similar to those of the spin-two graviton. Note also that  $\epsilon^\alpha$  is a polarization vector possessing the spacetime index  $\alpha$  ( $\alpha = 0, 1, 2, 3$ ) which is the same as the massive graviton spin index and is needed to incorporate minimally the spin DOF for the massive graviton. Next, as in the case of the GRB in the Dirac type relativistic massive photon model [12], the massive graviton could be interpreted as a spin-one GRB-like particle [14, 15]. The GRB-like graviton corresponding to its negative energy solution could then be regarded as an anti-graviton, which could be a candidate for an intense radiation flare of the GRB of GRB170817A [14, 15] associated with the binary compact objects merger event GW170817. Note that the massive anti-graviton could be described in terms of the massive gauge boson possessing a finite radius as in the massive photon in the stringy photon model [20]. For more details of the formalism of massive spin-one graviton, see Appendix C.

### III. GRAVITATIONAL WAVE RADIATION FROM MERGING BINARY COMPACT OBJECTS

In this section, in the MLGR we will investigate a binary system of merging compact objects which possesses masses  $M_1$  and  $M_2$  rotating on the  $x$ - $y$  plane. We assume that for simplicity the two compact objects  $M_1$  and  $M_2$  of equal mass  $M_1 = M_2 = M$  co-rotate in circular orbits of radius  $a$  about their common center of mass  $o$  with an angular frequency  $\omega$ , as shown in Figure 1(a). Note that the mass moves with *non-vanishing velocity*  $(v^i v^i)^{1/2} = \omega a$  along the tangential direction to the circular orbit as shown in Figure 1(a) which is consistent with the Wald approximation in the MLGR discussed in the previous section. Note also that the rotating binary compact objects can be thought of as the superposition of two oscillating binary compact objects, one along the  $x$ -axis and the other along the  $y$ -axis. The rotating mass vector  $\vec{M}(t)$  on the  $x$ - $y$  plane is given by

$$\vec{M}(t) = M(\hat{x} \cos \omega t + \hat{y} \sin \omega t). \quad (3.1)$$

For the masses on the  $x$ -axis and  $y$ -axis, exploiting (3.1) the Green retarded [1, 2] mass scalar potentials (or gravitational potentials)  $\phi_M^I$  and  $\phi_M^{II}$  are respectively given by

$$\begin{aligned} \phi_M^I(\vec{x}, t) &= -G \left( \frac{M \cos[\omega(t - R_+/c)]}{R_+} + \frac{M \cos[\omega(t - R_-/c)]}{R_-} \right), \\ \phi_M^{II}(\vec{x}, t) &= -G \left( \frac{M \sin[\omega(t - \bar{R}_+/c)]}{\bar{R}_+} + \frac{M \sin[\omega(t - \bar{R}_-/c)]}{\bar{R}_-} \right), \end{aligned} \quad (3.2)$$

where

$$\begin{aligned} R_\pm &= r \left( 1 \mp \frac{2a}{r} \sin \theta \cos \phi + \frac{a^2}{r^2} \right)^{1/2} = r \left( 1 \mp \frac{a}{r} \sin \theta \cos \phi \right), \\ \bar{R}_\pm &= r \left( 1 \mp \frac{2a}{r} \sin \theta \sin \phi + \frac{a^2}{r^2} \right)^{1/2} = r \left( 1 \mp \frac{a}{r} \sin \theta \sin \phi \right). \end{aligned} \quad (3.3)$$

Here we have used approximation  $a \ll r$ . For more details of  $R_\pm$ , see the geometry in Figure 1(b). After some algebra we arrive at the total contributions to the mass scalar potentials  $\phi_M = \phi_M^I + \phi_M^{II}$

$$\begin{aligned} \phi_M(\vec{x}, t) &= -\frac{2GM}{r} \left( \cos \left[ \omega \left( t - \frac{r}{c} \right) \right] + \sin \left[ \omega \left( t - \frac{r}{c} \right) \right] - \frac{\omega a^2}{cr} \sin^2 \theta \cos^2 \phi \sin \left[ \omega \left( t - \frac{r}{c} \right) \right] \right. \\ &\quad \left. + \frac{\omega a^2}{cr} \sin^2 \theta \sin^2 \phi \cos \left[ \omega \left( t - \frac{r}{c} \right) \right] \right), \end{aligned} \quad (3.4)$$

where we have ignored the much smaller terms exploiting approximation  $\frac{1}{r} \ll \frac{\omega}{c}$ . Note that the wavelength  $\lambda (= \frac{2\pi c}{\omega})$  of the GW is also much smaller than  $r$  to yield  $\lambda \ll r$ .

Next we construct the mass vector potential  $\vec{A}_M$  which is related with the mass current and is missing in the Newtonian gravity. Making use of (3.1) for the binary compact objects co-rotating on the  $x$ - $y$  plane, we find the mass current

$$\vec{I}_M(t) = -M\omega(\hat{x} \sin \omega t - \hat{y} \cos \omega t). \quad (3.5)$$

We then explicitly obtain the retarded mass vector potentials  $\vec{A}_M^I$  and  $\vec{A}_M^{II}$  for the mass current on the  $x$ -axis and  $y$ -axis

$$\begin{aligned} \vec{A}_M^I(\vec{x}, t) &= -\frac{GM\omega}{c^2} \left( \int_{-a}^0 \frac{\sin[\omega(t - R'_-/c)]}{R'_-} dx' - \int_0^{\bar{a}} \frac{\sin[\omega(t - R'_+/c)]}{R'_+} dx' \right) \hat{x}, \\ \vec{A}_M^{II}(\vec{x}, t) &= -\frac{GM\omega}{c^2} \left( -\int_{-a}^0 \frac{\cos[\omega(t - \bar{R}'_-/c)]}{\bar{R}'_-} dy' + \int_0^{\bar{a}} \frac{\cos[\omega(t - \bar{R}'_+/c)]}{\bar{R}'_+} dy' \right) \hat{y}, \end{aligned} \quad (3.6)$$

where  $R'_\pm$  and  $\bar{R}'_\pm$  are given by

$$R'_\pm = r \left( 1 \mp \frac{x'}{r} \sin \theta \cos \phi \right), \quad \bar{R}'_\pm = r \left( 1 \mp \frac{y'}{r} \sin \theta \sin \phi \right). \quad (3.7)$$

Here we also have exploited approximation  $a \ll r$ . For more details of  $R'_+$ , see the geometry in Figure 1(b). Note that  $\bar{a}$  in the upper bound of the second integral in (3.6) is the reduced radius from the origin after the mass  $M_1 (= M)$  travels during the half revolution. The distance  $\bar{a}$  is defined by

$$\delta a \equiv 2(a - \bar{a}), \quad (3.8)$$

so that  $\delta a$  can measure the distortion of the spirally merging binary compact objects during one cycle of their revolution. Note also that in the GW radiation phenomenology we assume that  $\delta a/a$  is extremely small to produce almost no stress in the two rotating mass compact objects. In the two body system of the rotating compact objects, the mass velocity  $(v^i v^i)^{1/2}$  ( $= a\omega$ ) is meaningful to implies that the Wald approximation in the MLGR defined in (2.25) and (2.26) is well proposed.

After some algebra associated with the definite integrations, we arrive at the total retarded mass vector potential  $\vec{A}_M = \vec{A}_M^I + \vec{A}_M^{II}$

$$\begin{aligned} \vec{A}_M(\vec{x}, t) &= -\frac{GM\omega\delta a}{2c^2r} \left[ \left( \sin \left[ \omega \left( t - \frac{r}{c} \right) \right] + \frac{\omega a}{c} \sin \theta \cos \phi \cos \left[ \omega \left( t - \frac{r}{c} \right) \right] \right) \hat{x} \right. \\ &\quad \left. + \left( -\cos \left[ \omega \left( t - \frac{r}{c} \right) \right] + \frac{\omega a}{c} \sin \theta \sin \phi \sin \left[ \omega \left( t - \frac{r}{c} \right) \right] \right) \hat{y} \right], \end{aligned} \quad (3.9)$$

where we have again used the approximations  $a \ll r$  and  $\lambda \ll r$  with  $\lambda$  being the GW wavelength. Note that, for the binary system of the two masses  $M_1 = M_2 = M$  of interest,<sup>2</sup> we obtain  $\bar{h}^{\alpha\beta}$  of the form

$$\bar{h}^{00} = -\frac{4}{c^2} \phi_M(\vec{x}, t), \quad \bar{h}^{0i} = -\frac{4}{c} A_M^i(\vec{x}, t), \quad \bar{h}^{ij} = 0, \quad (3.10)$$

where we have used (2.19), (2.22) and (2.24). Here  $\phi_M(\vec{x}, t)$  and  $A_M^i(\vec{x}, t)$  are given by (3.4) and (3.9), respectively. Using the relation  $h_{\alpha\beta} = \bar{h}_{\alpha\beta} - \frac{1}{2}\eta_{\alpha\beta}\bar{h}$  where  $\bar{h} = \eta^{\alpha\beta}\bar{h}_{\alpha\beta}$ , we can define the specific gravitational spacetime 4×4 metric tensor  $h_{\alpha\beta}$  ( $\alpha, \beta = 0, 1, 2, 3$ ) of the mass binary system.

Now exploiting (3.4) and (3.9), we find the mass electric field which also includes the mass vector potential effect  $\vec{E}_M \equiv -\nabla\phi_M - \frac{\partial\vec{A}_M}{\partial t} = E_M^r \hat{r} + E_M^\theta \hat{\theta} + E_M^\phi \hat{\phi}$  and the mass magnetic one  $\vec{B}_M \equiv \nabla \times \vec{A}_M = B_M^r \hat{\theta} + B_M^\phi \hat{\phi}$

$$\begin{aligned} E_M^r &= \frac{2GM\omega}{cr} \left( \sin \left[ \omega \left( t - \frac{r}{c} \right) \right] - \cos \left[ \omega \left( t - \frac{r}{c} \right) \right] \right), \\ E_M^\theta &= cB_M^\phi = \frac{GM\omega^2\delta a}{2c^2r} \cos \theta \left( \cos \left[ \omega \left( t - \frac{r}{c} \right) \right] \cos \phi + \sin \left[ \omega \left( t - \frac{r}{c} \right) \right] \sin \phi \right), \\ E_M^\phi &= -cB_M^\theta = \frac{GM\omega^2\delta a}{2c^2r} \left( -\cos \left[ \omega \left( t - \frac{r}{c} \right) \right] \sin \phi + \sin \left[ \omega \left( t - \frac{r}{c} \right) \right] \cos \phi \right), \end{aligned} \quad (3.11)$$

<sup>2</sup> This binary system phenomenology can be applicable to an isolated binary system of the particle masses  $M_1 = M_2 = M$ .

where we have included the relevant leading order terms. Exploiting (3.11), we find  $\vec{B}_M = \frac{1}{c}(\hat{r} \times \vec{E}_M)$  which implies that the  $\vec{E}_M$  and  $\vec{B}_M$  fields are mutually perpendicular, and are spherical waves (not plane waves) and their amplitudes decrease like  $1/r$  as they propagate. However, for large  $r$ , the GW waves are approximately plane waves over small regions, similar to the EM waves in (A.7) discussed in Appendix A. Note that the  $\vec{E}_M$  field possesses  $E_M^r \hat{r}$  component originated from the gravitational attraction from the binary compact objects. This characteristic is different from the rotating charge electric dipole moment system where  $E_Q^r \hat{r}$  component vanishes as in (A.7).

Next we formulate the mass Poynting vector in terms of  $\vec{E}_M$  and  $\vec{B}_M$  in (3.11)

$$\vec{S}_M \equiv \frac{c^2}{4\pi G}(\vec{E}_M \times \vec{B}_M) = \frac{c}{4\pi G} \left[ (E_M^\perp)^2 \hat{r} - E_M^r E_M^\perp \right], \quad (3.12)$$

where

$$\begin{aligned} \vec{E}_M^\perp &= E_M^\theta \hat{\theta} + E_M^\phi \hat{\phi}, \\ (E_M^\perp)^2 &= (E_M^\theta)^2 + (E_M^\phi)^2 = \left( \frac{GM\omega^2 \delta a}{2c^2 r} \right)^2 \left( 1 - \sin^2 \theta \cos^2 \left[ \omega \left( t - \frac{r}{c} \right) - \phi \right] \right). \end{aligned} \quad (3.13)$$

Note that the normalization factor  $\frac{c^2}{4\pi G}$  in (3.12) is systematically determined by using the proportionality constants  $-\frac{G}{c^2}$  of  $\vec{A}_M^I$  and  $\vec{A}_M^{II}$  in (3.6), and  $-G$  of  $\phi_M^I$  and  $\phi_M^{II}$  in (3.2) which is consistent with the Newtonian gravity [1, 18]. Note also that, in the optics associated with the massless spin-one graviton, the mass electric and mass magnetic fields  $\vec{E}_M$  and  $\vec{B}_M$  represent the two transverse directions of the GW, and the mass Poynting vector  $\vec{S}_M$  is parallel to the direction of the GW.

Using (3.12) and (3.13) we find the GW radiation intensity, namely the GW radiation power per surface  $\Sigma$ , which is obtainable by averaging in time over a complete cycle

$$\frac{dP_M}{d\Sigma} \equiv \langle \vec{S}_M \rangle = \frac{c}{4\pi G} \left( \frac{GM\omega^2 \delta a}{2c^2 r} \right)^2 \left( 1 - \frac{1}{2} \sin^2 \theta \right) \hat{r}. \quad (3.14)$$

Note that in (3.14) the  $\vec{E}_M^\perp$ -component of  $\vec{S}_M$  in (3.12) vanishes, after averaging in time over a complete cycle and then using  $\langle E_M^r \rangle = 0$ . To be specific, in the MLGR we find the non-vanishing  $\phi_M (= -\frac{c^2}{4} \bar{h}^{00})$  in (3.4) and the corresponding  $E_M^r \hat{r} = -\nabla \phi_M$  in (3.11). However, after averaging in time over a complete cycle, we have the vanishing contribution of  $\bar{h}^{00}$  to the *physical quantity*  $\langle E_M^r \rangle$  in the GW radiation algorithm. In this *phenomenological* sense, this aspect of  $\bar{h}^{00}$  in the Wald approximation in the MLGR is similar to that of  $\bar{h}_{TT}^{00} = 0$  in (3.17) in the TT gauge in the LGR, even though the gauge transformation in (2.34) in the MLGR vectorial algorithm is different from that in (2.4) in the LGR tensorial scheme. Moreover, we have another *phenomenological* characteristic that the two transverse directions of the GW are perpendicular to the GW radiation direction in the Wald approximation, similar to those in the LGR. Note also that, we have the vanishing contribution of  $E_M^r \hat{r}$  to the GW radiation intensity  $\frac{dP_M}{d\Sigma}$  in (3.14) by averaging in time over a complete cycle.

Now  $\frac{dP_M}{d\Sigma}$  has a maximum (minimum) value at  $\theta = 0$  ( $\theta = \frac{\pi}{2}$ ) to yield the invariant relation independent of the radial distance  $r$

$$\frac{dP_M}{d\Sigma}(\theta = 0) = 2 \frac{dP_M}{d\Sigma} \left( \theta = \frac{\pi}{2} \right), \quad (3.15)$$

implying that, at a given radial distance  $r$  from the origin of the binary system of compact objects, the GW radiation intensity on the revolution  $z$  axis of the compact objects is *twice* that on the equatorial  $x$ - $y$  plane where the compact objects locate. The characteristic invariant in (3.15) also occurs in the EM radiation intensity of the rotating charge electric dipole moment in (A.10). The geometrically invariant surface of the GW radiation intensity  $\frac{dP_M}{d\Sigma}$  then yields a prolate ellipsoid geometry in the corresponding intensity profile as shown in Figure 2.

The total GW radiation power constructed by integrating  $\langle \vec{S}_M \rangle$  over a sphere  $\Sigma_r$  of radius  $r$  is then given by

$$P_M \equiv \int \langle \vec{S}_M \rangle \cdot d\vec{\sigma} = \frac{GM^2 \omega^4 (\delta a)^2}{6c^3}, \quad (3.16)$$

where  $d\vec{\sigma}$  is an area element vector perpendicular to the surface  $\Sigma_r$ . As expected, the dimensionality of  $P_M$  is that of power, which is the same as the dimensionality of  $P_Q$  in (A.11). This aspect implies that the normalization factor  $\frac{c^2}{4\pi G}$  in (3.12) is well defined. Note that in the *ideal* binary compact objects without any distortion ( $\delta a = 0$ ) we obtain the vanishing total GW radiation power. In contrast, in the *physically merging* binary compact objects source we

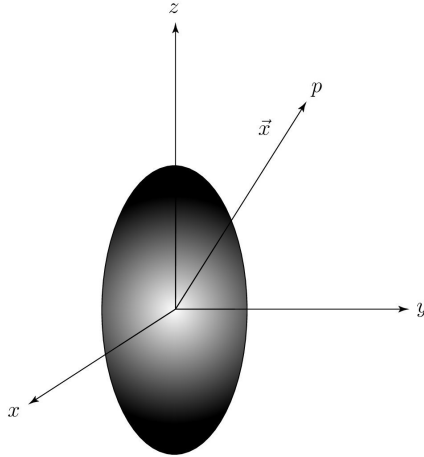


FIG. 2: The characteristic diagram for a surface of the GW radiation intensity  $\frac{dP_M}{d\Sigma}$  in (3.14), as a function of the polar angle  $\theta$ , showing a prolate ellipsoid geometry in the corresponding intensity profile. Here the binary compact objects reside on the equatorial  $x$ - $y$  plane as shown in Figure 1(a). Note that, at a given radial distance  $r = |\vec{x}|$  from the origin of the binary system of compact objects, the GW radiation intensity on the revolution  $z$  axis of the binary compact objects is twice that on the equatorial plane.

have the total power in (3.16) which is proportional to  $(\delta a)^2$ . Here  $\delta a$  is defined in (3.8). These phenomenological aspects of the distortion are consistent with the TT gauge approach to the merging binary compact objects [1, 2] in the LGR.

Now, it seems appropriate to comment on the TT gauge approach in the LGR, which is distinct from the MLGR defined in (2.20) and (2.24). First, for the LGR associated with merging binary compact objects of equal mass  $M$  which co-rotate in circular orbits of radius  $a$  about their common center of mass  $o$  with an angular frequency  $\omega$  as shown in Figure 1(a), we construct the symmetric second rank tensor for the GW radiation in the TT gauge [2]

$$\begin{aligned} \bar{h}_{TT}^{00} &= 0, \quad \bar{h}_{TT}^{0i} = 0, \\ \bar{h}_{TT}^{ij} &= \frac{8GM\omega^2 a^2}{c^4 r} \begin{pmatrix} \cos[2\omega(t - r/c)] & \sin[2\omega(t - r/c)] & 0 \\ \sin[2\omega(t - r/c)] & -\cos[2\omega(t - r/c)] & 0 \\ 0 & 0 & 0 \end{pmatrix}, \quad (i, j = 1, 2, 3). \end{aligned} \quad (3.17)$$

Note that the GW field  $\bar{h}_{TT}^{ij}$  in (3.17) represents spherical wave (not plane wave) and its amplitude decreases like  $1/r$  as it propagates, as in the case of  $\vec{E}_M$  and  $\vec{B}_M$  in (3.11) in the MLGR. In order to investigate the GW from binary compact objects in the LGR, we introduce the TT gauge [1, 2], and thus the GW originates from the second rank tensor  $\bar{h}_{TT}^{\alpha\beta}$  in (3.17). Using  $\bar{h}_{TT}^{\alpha\beta}$  in (3.17), in the TT gauge we find another condition

$$\bar{h}_{TT} = 0, \quad (3.18)$$

which yields

$$\bar{h}_{TT}^{\alpha\beta} = h_{TT}^{\alpha\beta}. \quad (3.19)$$

Exploiting (3.17) and (3.19), we can thus construct the spacetime metric  $g_{TT}^{\alpha\beta} = \eta^{\alpha\beta} + h_{TT}^{\alpha\beta}$  for (3.17).

Second, the GW radiation from the binary compact objects in the MLGR can be described in terms of the mathematically and physically independent vector  $\bar{h}^{0\alpha} = -\frac{4}{c} A_M^\alpha$  ( $\alpha = 0, 1, 2, 3$ ) in (2.20) and (2.24), without resorting to the second rank tensor  $\bar{h}_{TT}^{ij}$  in (3.17) in the LGR. Note also that the graviton possesses spin-one in the MLGR, but spin-two in the LGR, since the MLGR and LGR are delineated in terms of the vector  $\bar{h}^{0\alpha}$  related with  $\bar{h}^{ij} = 0$  in (2.19), and the second rank tensor  $\bar{h}_{TT}^{\alpha\beta}$  (especially the non-vanishing space-space components  $\bar{h}_{TT}^{ij}$  of the tensor in (3.17)), respectively.

Third, in the LGR the second rank tensor  $\bar{h}_{TT}^{ij}$  does not include the angle  $(\theta, \phi)$  dependences of  $A_M^i = -\frac{c}{4} \bar{h}^{0i}$  in (3.9) in the MLGR, which are related with those of the GW radiation intensity profile having a prolate ellipsoid geometry in Figure 2. To be more specific, formulating the components  $\bar{h}_{TT}^{ij}$  in (3.17) we have used the  $1/r$  factor and the retarded time  $t' = t - r/c$  without considering the  $(\theta, \phi)$  dependences of the vector  $\vec{x}$  shown in Figure 1(a). In contrast, in the Wald approximation in the MLGR, the angle dependences appear explicitly in the distances between the observation

point  $p$  and the masses  $M_1$  and  $M_2$  and also in the corresponding retarded time factors in  $\bar{h}^{00} = -\frac{4}{c^2}(\Phi_M^I + \Phi_M^{II})$ , as shown in (3.2) and (3.3) for instance.

Fourth, in the TT gauge, the DOF of  $\bar{h}_{TT}^{\alpha\beta}$  in (3.17) is two which is consistent with the corresponding DOF discussed in Section 2. Namely this DOF corresponds to two possible polarizations for plane GW associated with the massless spin-two graviton. Note that, for the massless plane GW traveling in the  $z$  direction, we find the GW four-vector  $k^\mu = (k, 0, 0, k)$  in (2.15). The traceless tensor  $\bar{h}_{TT}^{\alpha\beta}$  in (3.17) in the LGR then satisfies the transversality condition  $k_\mu \bar{h}_{TT}^{\mu\nu} = 0$ . Note also that, in the Wald approximation in the MLGR, the polarization vector  $\epsilon^\alpha = (0, \epsilon^1, \epsilon^2, 0)$  in (2.48) and the GW four-vector  $k^\mu = (k, 0, 0, k)$  in (2.45) satisfy the transversality condition  $k_\mu \epsilon^\mu = 0$  in (2.46). These aspects imply that the *phenomenology* of the LGR is similar to that in the Wald approximation in the sense that the two algorithms produce the transversality conditions (2.16) and (2.46) respectively, even though these algorithms are mathematically different to each other. For more details of the TT gauge, see Appendix B.

#### IV. CONCLUSIONS

In summary, we have formulated the MLGR where the mass scalar potential has the additional dynamical DOF. In the static gravitational field limit of the MLGR, the mass scalar potential is consistent with the well-established gravitational potential in the Newtonian gravity. Next we also have found that the MLGR allows the mass vector potential which originates from the mass current and is missing in the Newtonian gravity. As an application of the MLGR, we have investigated the phenomenological aspects of the merging binary compact objects which co-rotate in circular orbits about their common center of mass with a constant angular frequency. To be specific, we have constructed the mass scalar and mass vector potentials of the merging binary compact objects at an observation point located far away from the compact objects. We then have formulated the mass electric and mass magnetic fields, and the mass Poynting vector. Next we have found the GW radiation intensity profile having a prolate ellipsoid geometry due to the merging binary compact objects source, and then explicitly obtained the total GW radiation power due to the source. We also have observed that, in no distorting limit of the binary compact objects, they do not yield the total GW radiation power, which is consistent with the TT gauge approach in the LGR. Note that the MLGR related with  $\bar{h}^{00} = -\frac{4}{c^2}\phi_M$  is consistently reduced to the Newtonian gravity having  $\nabla^2\phi_M = 4\pi G\rho_M$  in the static limit, differently from the TT gauge approach with  $\bar{h}_{TT}^{00} = 0$ . This fact implies that the gauge in the MLGR is applicable to both the GW radiation and Newtonian gravity simultaneously. Recently the galaxy-based observatories have been proposed [8] and thus the angle  $(\theta, \phi)$  dependence of the GW radiation depicted in Figure 1(a), which is not explained in the TT gauge, could become important increasingly in the astrophysical phenomenology. To be specific, the MLGR constructed in this work could be exploited in the future experimental instruments, which could detect the angle dependence of the GW radiation power from the merging binary compact objects. The MLGR algorithm for the angle dependence of the GW could then play a role in the realistic *precision astrophysics*. One of the main points of this paper is that, in the MLGR we have found the mathematically and physically well defined spin-one graviton, distinct from the second rank tensor algorithm in the LGR which could allow the spin-two graviton. It will be interesting to search for the spin-one graviton which could be related with the well-established spin-one photon phenomenology such as the photoelectric effect and Compton scattering for instance. Once this is done, the MLGR algorithm associated with the graviton could give some progress impacts on the precision astrophysics. Assuming the possibility of the *massive* spin-one graviton, we have observed that the massive graviton would be interpreted as a GRB-like graviton, which could then be regarded as an anti-graviton. This anti-graviton could be phenomenologically a candidate for an *intense radiation flare* of the GRB170817A related with the *binary compact objects merger event* GW170817. Finally we have shown that the spin-one graviton in the MLGR has two polarization DOF whose aspect is shared by the spin-two graviton in the LGR.

#### Acknowledgments

The author would like to thank the anonymous referees for helpful comments. He was supported by Basic Science Research Program through the National Research Foundation of Korea funded by the Ministry of Education, NRF-2019R1I1A1A01058449.

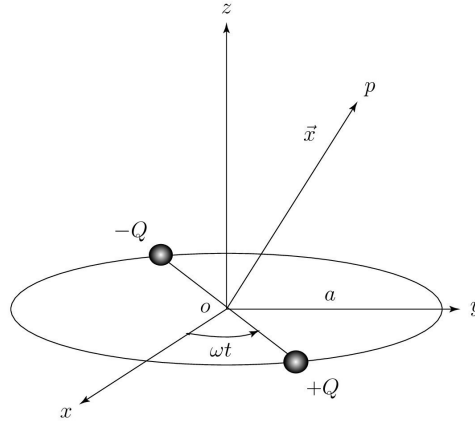


FIG. 3: The schematic diagram for a rotating charge electric dipole moment consisting of charges  $+Q$  and  $-Q$  which co-rotate in circular orbits of radius  $a$ , with an angular frequency  $\omega$ .

### Appendix A: EM wave radiation from rotating charge electric dipole moment

In this appendix we will pedagogically investigate the charge electric dipole moment [19, 21, 22] which possesses charges  $+Q$  and  $-Q$  rotating on the  $x$ - $y$  plane. Here the charge electric dipole moment is not merging to yield no distortion. We assume that for simplicity the two charges co-rotate in circular orbits of radius  $a$  about their common center of mass  $o$  with an angular frequency  $\omega$ , as shown in Figure 3. Note that the rotating charge electric dipole can be thought of as the superposition of two oscillating charge electric dipoles, one along the  $x$ -axis and the other along the  $y$ -axis [22]. The rotating charge vector  $\vec{Q}(t)$  on the  $x$ - $y$  plane is given by

$$\vec{Q}(t) = Q(\hat{x} \cos \omega t + \hat{y} \sin \omega t). \quad (\text{A.1})$$

For the charges on the  $x$ -axis and  $y$ -axis, exploiting (A.1) we obtain the Green retarded charge scalar potential  $\phi_Q^I$  and  $\phi_Q^{II}$ , respectively

$$\begin{aligned} \phi_Q^I(\vec{x}, t) &= \frac{1}{4\pi\epsilon_0} \left( \frac{Q \cos[\omega(t - R_+/c)]}{R_+} - \frac{Q \cos[\omega(t - R_-/c)]}{R_-} \right), \\ \phi_Q^{II}(\vec{x}, t) &= \frac{1}{4\pi\epsilon_0} \left( \frac{Q \sin[\omega(t - \bar{R}_+/c)]}{\bar{R}_+} - \frac{Q \sin[\omega(t - \bar{R}_-/c)]}{\bar{R}_-} \right), \end{aligned} \quad (\text{A.2})$$

where  $R_{\pm}$  and  $\bar{R}_{\pm}$  are given by (3.3). Here the subscript  $Q$  stands for the charge related quantities. Following the technical procedures similar to those in Section 3, we find the total contributions to the charge scalar potentials  $\phi_Q = \phi_Q^I + \phi_Q^{II}$

$$\phi_Q(\vec{x}, t) = -\frac{Q\omega a}{2\pi\epsilon_0} \left( \frac{\sin \theta}{cr} \right) \left( \cos \phi \sin \left[ \omega \left( t - \frac{r}{c} \right) \right] - \sin \phi \cos \left[ \omega \left( t - \frac{r}{c} \right) \right] \right), \quad (\text{A.3})$$

where we have used approximations  $a \ll r$  and  $\frac{1}{r} \ll \frac{\omega}{c}$ , implying that the wavelength  $\lambda (= \frac{2\pi c}{\omega})$  of the EM wave is much smaller than  $r$  to yield  $\lambda \ll r$ .

Making use of (A.1) for the charges co-rotating on the  $x$ - $y$  plane, we find the charge current

$$\vec{I}_Q(t) = -Q\omega(\hat{x} \sin \omega t - \hat{y} \cos \omega t). \quad (\text{A.4})$$

Next we find the retarded charge vector potentials  $\vec{A}_Q^I$  and  $\vec{A}_Q^{II}$  for the charge currents on the  $x$ -axis and the  $y$ -axis, respectively

$$\begin{aligned} \vec{A}_Q^I(\vec{x}, t) &= \frac{\mu_0 Q \omega}{4\pi} \left( - \int_{-a}^0 \frac{\sin[\omega(t - R'_-/c)]}{R'_-} dx' - \int_0^a \frac{\sin[\omega(t - R'_+/c)]}{R'_+} dx' \right) \hat{x}, \\ \vec{A}_Q^{II}(\vec{x}, t) &= \frac{\mu_0 Q \omega}{4\pi} \left( \int_{-a}^0 \frac{\cos[\omega(t - \bar{R}'_-/c)]}{\bar{R}'_-} dy' + \int_0^a \frac{\cos[\omega(t - \bar{R}'_+/c)]}{\bar{R}'_+} dy' \right) \hat{y}, \end{aligned} \quad (\text{A.5})$$

where  $R'_\pm$  and  $\bar{R}'_\pm$  are given by (3.7). Here we have used the approximations  $a \ll r$  and  $\frac{1}{r} \ll \frac{\omega}{c}$ . Note that in (A.2) and (A.5) we have used the charges  $(+Q, -Q)$ , distinct from the binary system of compact objects where we have exploited the masses  $(M, M)$  in (3.2) and (3.6). Exploiting the charge vector potentials in (A.5), we obtain the total retarded charge vector potential  $\vec{A}_Q = \vec{A}_Q^I + \vec{A}_Q^{II}$

$$\begin{aligned} \vec{A}_Q(\vec{x}, t) = & \frac{\mu_0 Q \omega a}{2\pi r} \left[ -\left( \sin \left[ \omega \left( t - \frac{r}{c} \right) \right] + \frac{\omega a}{2c} \sin \theta \cos \phi \cos \left[ \omega \left( t - \frac{r}{c} \right) \right] \right) \hat{x}, \right. \\ & \left. + \left( \cos \left[ \omega \left( t - \frac{r}{c} \right) \right] - \frac{\omega a}{2c} \sin \theta \sin \phi \sin \left[ \omega \left( t - \frac{r}{c} \right) \right] \right) \hat{y} \right]. \end{aligned} \quad (\text{A.6})$$

Now using (A.3) and (A.6), we find the charge electric field  $\vec{E}_Q \equiv -\nabla \phi_Q - \frac{\partial \vec{A}_Q}{\partial t} = E_Q^\theta \hat{\theta} + E_Q^\phi \hat{\phi}$  and charge magnetic one  $\vec{B}_Q \equiv \nabla \times \vec{A}_Q = B_Q^\theta \hat{\theta} + B_Q^\phi \hat{\phi}$

$$\begin{aligned} E_Q^\theta &= c B_Q^\phi = \frac{\mu_0 Q \omega^2 a}{2\pi r} \cos \theta \left( \cos \left[ \omega \left( t - \frac{r}{c} \right) \right] \cos \phi + \sin \left[ \omega \left( t - \frac{r}{c} \right) \right] \sin \phi \right), \\ E_Q^\phi &= -c B_Q^\theta = \frac{\mu_0 Q \omega^2 a}{2\pi r} \left( -\cos \left[ \omega \left( t - \frac{r}{c} \right) \right] \sin \phi + \sin \left[ \omega \left( t - \frac{r}{c} \right) \right] \cos \phi \right), \end{aligned} \quad (\text{A.7})$$

where we have included the relevant leading terms. From (A.7), we obtain  $\vec{B}_Q = \frac{1}{c}(\hat{r} \times \vec{E}_Q)$ . Note that  $\vec{E}_Q$  does not have the  $E_Q^r$  component, different from the  $\vec{E}_M$  of the binary compact objects which possesses the  $E_M^r$  component in (3.11).

Next we formulate the charge Poynting vector in terms of  $\vec{E}_Q$  and  $\vec{B}_Q$  in (A.7)

$$\vec{S}_Q \equiv \frac{1}{\mu_0} (\vec{E}_Q \times \vec{B}_Q) = \frac{1}{\mu_0 c} (E_Q)^2 \hat{r} \quad (\text{A.8})$$

where

$$(E_Q)^2 = (E_Q^\theta)^2 + (E_Q^\phi)^2 = \left( \frac{\mu_0 Q \omega^2 a}{2\pi r} \right)^2 \left( 1 - \sin^2 \theta \cos^2 \left[ \omega \left( t - \frac{r}{c} \right) - \phi \right] \right). \quad (\text{A.9})$$

Now, using (A.8) and (A.9) and averaging in time over a complete cycle, we arrive at the EM radiation intensity, namely the EM radiation power per surface  $\Sigma$

$$\frac{dP_Q}{d\Sigma} \equiv \langle \vec{S}_Q \rangle = \frac{1}{\mu_0 c} \left( \frac{\mu_0 Q \omega^2 a}{2\pi r} \right)^2 \left( 1 - \frac{1}{2} \sin^2 \theta \right) \hat{r}. \quad (\text{A.10})$$

The total EM radiation power constructed by integrating  $\langle \vec{S}_Q \rangle$  over a sphere  $\Sigma_r$  of radius  $r$  is then given by

$$P_Q \equiv \int \langle \vec{S}_Q \rangle \cdot d\vec{\sigma} = \frac{2\mu_0 Q^2 \omega^4 a^2}{3\pi c}, \quad (\text{A.11})$$

where  $d\vec{\sigma}$  is an area element vector perpendicular to the surface  $\Sigma_r$ . Note that the total EM radiation power  $P_Q$  in (A.11) for the rotating charge electric dipole moment on the  $x$ - $y$  plane is twice that for the oscillating charge electric dipole moment along the  $x$ -direction, assuming the same time dependence possessing an angular frequency  $\omega$  of these rotating and oscillating cases.

## Appendix B: TT gauge for rotating binary compact objects

In this appendix we will address brief comments on the TT gauge [1–3] for wave radiation from rotating binary system related with (3.17). To accomplish this, we first introduce the TT gauge which is defined by choosing [2]

$$\bar{h}_{TT}^{0i} \equiv 0 \quad \text{and} \quad \bar{h}_{TT} \equiv 0. \quad (\text{B.1})$$

Here the second condition in (B.1) implies that  $\bar{h}_{TT}^{\alpha\beta} = h_{TT}^{\alpha\beta}$  in (3.19).

Next we study the space-space component of  $\bar{h}_{TT}^{ij}$ , which is given by the integrated stress within the source. Note that this stress may be described in terms of the quadrupole moment in the TT gauge. Now we define the quadrupole moment tensor for the source as follows [1–3]

$$I^{ij}(t) = \int T^{00} x^i x^j d^3 x, \quad (\text{B.2})$$

where  $x^i = (x, y, z)$ . Together with the relation  $T^{00} = c^2 \rho_M(\vec{x}, t)$ , (B.2) produces

$$I^{ij}(t) = c^2 \int \rho_M(\vec{x}, t) x^i x^j d^3 x. \quad (\text{B.3})$$

We assume for simplicity that the mass orbits reside on the  $x$ - $y$  plane as shown in Figure 1(a). Exploiting the geometry in Figure 1(a), we read off the coordinates of  $\vec{x}(M_1)$  and  $\vec{x}(M_2)$ :

$$\vec{x}(M_1) = (a \cos \omega t, a \sin \omega t, 0), \quad \vec{x}(M_2) = (-a \cos \omega t, -a \sin \omega t, 0), \quad (\text{B.4})$$

to yield the mass density

$$\rho_M(\vec{x}, t) = M[\delta(x^1 - a \cos \omega t) \delta(x^2 - a \sin \omega t) + \delta(x^1 + a \cos \omega t) \delta(x^2 + a \sin \omega t)] \delta(x^3). \quad (\text{B.5})$$

Inserting  $\rho_M(\vec{x}, t)$  in (B.5) into (B.3) we arrive at

$$I^{ij}(t) = M c^2 a^2 \begin{pmatrix} 1 + \cos(2\omega t) & \sin(2\omega t) & 0 \\ \sin(2\omega t) & 1 + \cos(2\omega t) & 0 \\ 0 & 0 & 0 \end{pmatrix}. \quad (\text{B.6})$$

Next we find  $\bar{h}_{TT}^{ij}$  in terms of the quadrupole moment tensor  $I^{ij}(t)$  [1–3]

$$\bar{h}_{TT}^{ij} = -\frac{2G}{c^6 r} \frac{d^2 I^{ij}(t)}{dt^2} \Big|_{\text{retarded}}, \quad (\text{B.7})$$

where the derivative is evaluated at the retarded time  $t' = t - r/c$ . Combining the quadrupole moment tensor in (B.6) and  $\bar{h}_{TT}^{ij}$  in (B.7) we end up with

$$\bar{h}_{TT}^{ij} = \frac{8G M a^2 \omega^2}{c^4 r} \begin{pmatrix} \cos[2\omega(t - r/c)] & \sin[2\omega(t - r/c)] & 0 \\ \sin[2\omega(t - r/c)] & -\cos[2\omega(t - r/c)] & 0 \\ 0 & 0 & 0 \end{pmatrix}, \quad (i, j = 1, 2, 3). \quad (\text{B.8})$$

which reproduces  $\bar{h}_{TT}^{ij}$  in (3.17).

Now we study the time-time component of  $\bar{h}_{TT}^{00}$ . To do this we first consider the one-body object of mass  $M$  located at the position  $o$  in Figure 1(a). We then find the potential  $\bar{h}^{00}$  as follows

$$\bar{h}^{00} = \frac{4GM}{c^2 r}. \quad (\text{B.9})$$

For the radiative part  $\bar{h}_{TT}^{00}$  of the two-body system of interest, we find [2]

$$\bar{h}_{TT}^{00} = 0, \quad (\text{B.10})$$

which, together with (B.1) and (B.8), yields (3.17). Note that the first condition in the TT gauge in (B.1) cannot explain the DOF of the non-vanishing mass current density associated with the mass velocity  $v^i (\neq 0)$  and the ensuing  $J_M^i \equiv \rho_M v^i$  which is explicitly included in the Wald approximation in the MLGR in the gravitational wave radiation phenomenology in Sections 2 and 3.

### Appendix C: Formalism of massive spin-one graviton

In this appendix we will study the formulation of a *massive* graviton in the relativistic quantum mechanics (RQM). Note that the photon has been known to be massive in the stringy photon model [20]. Note also that, in the massless limit, the graviton has the same physical and mathematical structures as the photon as shown in (2.36). Since the

formulation of the Hamiltonian in the RQM for a massive photon has been well-established [12], we will follow this algorithm to investigate the massive graviton. To do this, for simplicity we assume that the graviton trajectory is a straight line along the  $z$  direction. Exploiting  $E^2 = m^2 + p^2$  where  $p = p_z = |\vec{p}|$ , we find the relativistic equation of motion for the massive graviton given by<sup>3</sup>

$$H\phi^a = i\partial_0\phi^a. \quad (\text{C.1})$$

Now we include a possibility of a negative energy solution for the massive graviton in this work, by following the formalism for the massive photon. For the corresponding Hamiltonian for the massive graviton, we introduce a minimal  $2 \times 2$  matrix associated with the positive and negative energy solutions. Next, following the RQM for the massive photon, we proceed to find  $H$  in (C.1) for the massive graviton. The Hamiltonian  $H$  is then given by a  $2 \times 2$  matrix acting on the component index  $A$  only

$$H = \vec{\mathcal{A}} \cdot \vec{p} + \mathcal{B}m, \quad (\text{C.2})$$

where  $\mathcal{A}_i$  ( $i = 1, 2, 3$ ) and  $\mathcal{B}$  are  $2 \times 2$  matrices. Making use of  $E^2 = m^2 + p^2$ , we obtain the algebra between  $\mathcal{A}_i$  and  $\mathcal{B}$ :

$$\{\mathcal{A}_i, \mathcal{A}_j\} = 2\delta_{ij}I, \quad \mathcal{B}^2 = I, \quad \{\mathcal{A}_i, \mathcal{B}\} = 0, \quad \mathcal{A}_i^\dagger = \mathcal{A}_i, \quad \mathcal{B}^\dagger = \mathcal{B}, \quad (\text{C.3})$$

where  $I$  is a  $2 \times 2$  unit matrix. Note that eigenvalues of  $\mathcal{A}_i$  or  $\mathcal{B}$  are  $\pm 1$  and  $\text{tr}\mathcal{A}_i = \text{tr}\mathcal{B} = 0$ .

As in the RQM for the massive photon, exploiting the above relations in (C.3) and the massive graviton Hamiltonian in (C.2), we find the representations for  $\mathcal{A}_i$  and  $\mathcal{B}$  given by  $\mathcal{A}_1 = \mathcal{A}_2 = 0$ ,  $\mathcal{A}_3 = \sigma_1$  and  $\mathcal{B} = \sigma_3$ , where  $\sigma_i$  are the Pauli matrices. Inserting the above representations for  $\mathcal{A}_i$  and  $\mathcal{B}$  into (C.2), we obtain the  $2 \times 2$  Hamiltonian:

$$H = \begin{pmatrix} m & -i\partial_3 \\ -i\partial_3 & -m \end{pmatrix}. \quad (\text{C.4})$$

Making use of (C.1) and (C.4), we find the relativistic equation of motion for the massive graviton

$$(i\Gamma^\mu\partial_\mu - m)\phi^a(x) = 0, \quad (\text{C.5})$$

where  $\phi^a(x)$  is a function of  $x^\mu$  and  $\Gamma^\mu$  is given by  $\Gamma^\mu = (\sigma_3, 0, 0, i\sigma_2)$ .

Now we investigate the phenomenological aspects of the RQM for the massive graviton. To do this, we start with the equation in (C.5). Since, for the relativistic massive graviton satisfying the relation  $E^2 = m^2 + p^2$ , we have two kinds of solutions corresponding to  $E = \pm(m^2 + p^2)^{1/2} \equiv \pm p_0$ , we introduce an ansatz for the wave function  $\phi^a$ :

$$\phi^a(x) = \phi^a(p^\mu)e^{\mp ip_\sigma x^\sigma}, \quad (\text{C.6})$$

for the positive and negative solutions with the upper and lower signs, respectively.

Next we find the positive energy solution  $\phi_+^a(x)$  with  $E > 0$  and the negative energy solution  $\phi_-^a(x)$  with  $E = -|E| < 0$ , respectively,

$$\phi_+^a(x) = u^a(p^\mu)e^{-ip_\sigma x^\sigma}, \quad \phi_-^a(x) = v^a(p^\mu)e^{+ip_\sigma x^\sigma}, \quad (\text{C.7})$$

where  $u^a(p^\mu)$  and  $v^a(p^\mu)$  are given by

$$u^a(p^\mu) = \epsilon^a \left( \frac{E + m}{2m} \right)^{1/2} \begin{pmatrix} 1 \\ \frac{p}{E+m} \end{pmatrix}, \quad v^a(p^\mu) = \epsilon^a \left( \frac{|E| + m}{2m} \right)^{1/2} \begin{pmatrix} \frac{p}{|E|+m} \\ 1 \end{pmatrix}. \quad (\text{C.8})$$

Here  $\epsilon^a$  is a unit polarization vector having the spacetime index  $a$  ( $a = 0, 1, 2, 3$ ) which is the same as the spin index and is needed to incorporate minimally the spin DOF for the massive graviton. Here we have considered the Lorentz

---

<sup>3</sup> Here  $\phi^a$  stands for the wave function for the massive graviton, explicitly given by  $\phi_A^a = (\phi_1^a, \phi_2^a)^T$  where the superscript  $T$  denotes the transpose of the wave function components. Here the spin index  $a$  ( $a = 0, 1, 2, 3$ ) denotes the spin DOF for the massive graviton with spin one. The component index  $A$  ( $A = 1, 2$ ) stands for the two DOF which have the same DOF of the positive and negative energy solutions with the energy index  $\pm$  in (C.7), since the positive and negative energy solutions are given by linear combinations of the two wave functions with the component indices. Note that the wave function  $\phi_A^a$  is described in terms of a  $1 \times (2_{\text{energy}} \otimes 4_{\text{spin}}) = 1 \times 8$  column vector. From now on, for simplicity we will drop the index  $A$  in the wave functions except (C.10).

frame where  $\epsilon^a$  is purely space-like so that we can readily find that  $\epsilon^a \epsilon^a = \vec{\epsilon} \cdot \vec{\epsilon} = 1$ , or  $\epsilon_a \epsilon^a = -\vec{\epsilon} \cdot \vec{\epsilon} = -1$ . Next we have the relation  $p_a \epsilon^a \neq 0$ ,<sup>4</sup> since for the massive graviton we have longitudinal component in addition to transverse ones, similar to the phonon associated with massive particle lattice vibrations [17]. In the RQM for the photon, we have the photon and anti-photon corresponding to the positive and negative energy solutions, respectively. Similar to the RQM for the photon, we have the massive graviton with negative energy solution.

Reshuffling the equation of motion in (C.5) we obtain with  $\bar{\phi}^a \equiv \phi^{a\dagger} \Gamma^0$

$$i\sigma_3 \partial_0 \phi^a - \sigma_2 \partial_3 \phi^a - m \phi^a = 0, \quad i\partial_0 \bar{\phi}^a \sigma_3 - \partial_3 \bar{\phi}^a \sigma_2 + m \bar{\phi}^a = 0, \quad (C.9)$$

with which we find the probability continuity equation  $\partial_0 \rho + \nabla \cdot \vec{J} = 0$ , where the probability density  $\rho$  and probability current  $\vec{J}$  are given by

$$\rho \equiv \bar{\phi}^a \sigma_3 \phi^a = \phi^{a\dagger} \phi^a = \phi_1^* \phi_1 + \phi_2^* \phi_2, \quad \vec{J} \equiv \bar{\phi}^a (i\sigma_2) \phi^a \hat{z} = \phi^{a\dagger} \sigma_1 \phi^a \hat{z} = (\phi_1^* \phi_2 + \phi_2^* \phi_1) \hat{z}. \quad (C.10)$$

Here we have used the notation  $\phi^a \equiv \epsilon^a(\phi_1, \phi_2)^T$ . Note that the probability density  $\rho$  is positive definite in the RQM for the massive graviton. For the positive energy solution with  $E > 0$ , inserting  $\phi_+^a(x)$  in (C.7) into  $\rho$  and  $\vec{J}$  in (C.10), we obtain  $\rho = \frac{E}{m}$  and  $\vec{J} = \frac{\vec{p}}{m}$ . For the negative energy solution with  $E = -|E| < 0$  where  $|E| = (m^2 + p^2)^{1/2}$ , inserting  $\phi_-^a(x)$  in (C.7) into  $\rho$  and  $\vec{J}$ , we find  $\rho = \frac{|E|}{m}$  and  $\vec{J} = \frac{\vec{p}}{m}$ .

It seems appropriate to comment on the negative energy solution  $\phi_-^a$  in the RQM for the massive graviton. First, for the negative energy solution of the massive graviton, since we have  $\rho = |\phi_1|^2 + |\phi_2|^2 > 0$ ,  $\rho = \frac{|E|}{m}$  implies that  $m$  is positive. Even in this negative energy solution, the positive mass  $m$  moves with the probability current  $\vec{J}$  along the  $z$  direction. From now on, we will name the graviton possessing the properties that the particle has the positive mass  $m$  and positive energy  $|E|$  and is associated with the negative energy solution, an *anti-graviton*.

Second, we propose that the anti-graviton related with the negative energy solution is defined to interact repulsively with the ordinary massive graviton, oppositely to the ordinary massive graviton-graviton attractive gravitational interaction pattern. Note that, in the Dirac RQM, the positron associated with the negative energy solution is defined to interact attractively with the electron, oppositely to the ordinary charged electron-electron repulsive electromagnetic interaction pattern. The same logic can be applied to the gravitational interaction case related with the anti-graviton. Next, the positron and electron can annihilate each other via the particle and anti-particle pair annihilation mechanism. In contrast, the uncharged anti-graviton scatters away from the ordinary massive particle including the graviton and photon, in the repulsive gravitational interaction between the anti-graviton and the ordinary massive particle.

Third, since the anti-graviton is repulsive against charged or uncharged ordinary massive matters, the anti-graviton does not adhere to the ordinary massive matters, so that the anti-gravitons can produce an intense radiation flare of the GRB-like graviton. Phenomenologically this anti-graviton could be a candidate for an intense radiation flare of the GRB170817A related with the binary compact objects merger event GW170817.

---

[1] R.M. Wald, *General Relativity* (University of Chicago Press, Chicago, 1984)

[2] M.P. Hobson, G. Efstathiou and A.N. Lasenby, *General Relativity: An Introduction for Physicists* (Cambridge University Press, Cambridge, 2006)

[3] S.M. Carroll, *An Introduction to General Relativity: Spacetime and Geometry* (Addison Wesley, San Francisco, 2004)

[4] M. Fierz and W. Pauli, *Relativistic wave equations for particles of arbitrary spin in an electromagnetic field*, Proc. Roy. Soc. Lond. A **173**, 211 (1939)

[5] [LIGO Scientific Collaboration] J. Aasi et al., *Advanced LIGO*, Class. Quant. Grav. **32**, 074001 (2015)

[6] D. Reitze, R.X. Adhikari, S. Ballmer, B. Barish, L. Barsotti, G. Billingsley, D.A. Brown, Y. Chen, D. Coyne, R. Eisenstein, M. Evans, P. Fritschel, E.D. Hall, A. Lazzarini, G. Lovelace, J. Read, B.S. Sathyaprakash, D. Shoemaker, J. Smith, C. Torrie, S. Vitale, R. Weiss, C. Wipf and M. Zucker, *Cosmic explorer: the U.S. contribution to gravitational-wave astronomy beyond LIGO*, Bull. Am. Astron. Soc. **51**, 35 (2019)

[7] [LIGO Scientific Collaboration, VIRGO Collaboration, and KAGRA Collaboration] R. Abbott et al., *Observation of Gravitational Waves from Two Neutron Star-Black Hole Coalescences*, Astrophys. J. Lett. **915**, L5 (2021)

[8] S. Dandapat, M. Ebersold, A. Susobhanan, P. Rana, A. Gopakumar, S. Tiwari, M. Haney, H.M. Lee and N. Kolhe, *Gravitational waves from black-hole encounters: Prospects for ground and galaxy-based observatories*, Phys. Rev. D **108**, 024013 (2023)

---

<sup>4</sup> Here we use the units of  $\hbar = 1$  to yield  $p^\mu = \hbar k^\mu = k^\mu$  and  $p_\mu \epsilon^\mu = k_\mu \epsilon^\mu \neq 0$  as in (2.49).

- [9] S. Jana, S.J. Kapadia, T. Venumadhav and P. Ajith, *Cosmography using strongly lensed gravitational waves from binary black holes*, Phys. Rev. Lett. **130**, 261401 (2023)
- [10] R.W. Klebesadel, I.B. Strong and R.A. Olson, *Observations of gamma-ray bursts of cosmic origin*, Astrophys. J. Lett. **182**, L85 (1973)
- [11] D. Svinkin, D. Frederiks, K. Hurley, R. Aptekar, S. Golenetskii, A. Lysenko, A.V. Ridnaia, A. Tsvetkova, M. Ulanov, T.L. Cline, I. Mitrofanov, D. Golovin, A. Kozyrev, M. Litvak, A. Sanin, A. Goldstein, M.S. Briggs, C. Wilson-Hodge, A. von Kienlin, X.L. Zhang, A. Rau, V. Savchenko, E. Bozzo, C. Ferrigno, P. Ubertini, A. Bazzano, J.C. Rodi, S. Barthelmy, J. Cummings, H. Krimm, D.M. Palmer, W. Boynton, C.W. Fellows, K.P. Harshman, H. Enos and R. Starr, *A bright gamma-ray flare interpreted as a giant magnetar flare in NGC 253*, Nature **589**, 211 (2021)
- [12] S.T. Hong, *Dirac type relativistic quantum mechanics for massive photons*, Nucl. Phys. B **980**, 115852 (2022)
- [13] [LIGO Scientific and Virgo Collaborations] B.P. Abbott et al., *GW170817: Observation of gravitational waves from a binary neutron star inspiral*, Phys. Rev. Lett. **119**, 161101 (2017)
- [14] [LIGO Scientific and Virgo and Fermi-GBM and INTEGRAL Collaborations] B.P. Abbott et al., *Gravitational waves and gamma-rays from a binary neutron star merger: GW170817 and GRB 170817A*, Astrophys. J. Lett. **848**, L13 (2017)
- [15] A. Goldstein, P. Veres, E. Burns, M.S. Briggs, R. Hamburg, D. Kocevski, C.A. Wilson-Hodge, R.D. Preece, S. Poolakkil, O.J. Roberts, C. M. Hui, V. Connaughton, J. Racusin, A. von Kienlin, T.D. Canton, N. Christensen, T. Littenberg, K. Siellez, L. Blackburn, J. Broida, E. Bissaldi, W.H. Cleveland, M.H. Gibby, M.M. Giles, R.M. Kippen, S. McBreen, J. McEnerly, C.A. Meegan, W.S. Paciesas and M. Stanbro, *An ordinary short gamma-ray burst with extraordinary implications: fermi-GBM detection of GRB 170817A*, Astrophys. J. Lett. **848**, L14 (2017)
- [16] V.M. Kaspi and A. Beloborodov, *Magnetars*, Ann. Rev. Astron. Astrophys. **55**, 261 (2017)
- [17] N.W. Ashcroft and N.D. Mermin, *Solid State Physics* (Brooks/Cole, London, 1976)
- [18] H. Goldstein, *Classical Mechanics* (Addison-Wesley, London, 1980)
- [19] J.D. Jackson, *Classical Electrodynamics* (John Wiley & Sons, Danvers, MA, 1999)
- [20] S.T. Hong, *Photon intrinsic frequency and size in stringy photon model*, Nucl. Phys. B **976**, 115720 (2022)
- [21] W.E. Baylis, *Electrodynamics: A Modern Geometric Approach* (Birkhäuser, Boston, 2002)
- [22] D.J. Griffiths, *Introduction to Electrodynamics* (Prentice Hall, Upper Saddle River, NJ, 1999)